Skeletal Radiology (2019) 48:527–534
https://doi.org/10.1007/s00256-018-3058-6

SCIENTIFIC ARTICLE

Correlation of bone marrow cellularity and metabolic activity in healthy volunteers with simultaneous PET/MR imaging

Takeshi Fukuda[1] · Mingqian Huang[1] · Anuradha Janardhanan[1] · Mark E. Schweitzer[1] · Chuan Huang[1,2]

Received: 21 May 2018 / Revised: 21 August 2018 / Accepted: 27 August 2018 / Published online: 7 September 2018

Abstract

Objective To evaluate the correlation between bone marrow cellularity (BMC) and metabolic activity in healthy subjects and to see whether yellow marrow is indeed metabolically quiescent. Because metabolic activity can be assumed to reflect vascularity, we assessed the relationship between regional metabolic activity and geographic frequency of metastases as noted in the literature.
Materials and methods Two hundred and twenty locations (ten in each side of the pelvis and proximal femur) were evaluated in 11 consecutive healthy volunteers with simultaneous PET/MR. BMC was calculated through precise water–fat fraction quantification with a 6-echo gradient echo. We analyzed correlations between cellularity and SUVr, age, and R2*. We also looked at the relation between our results and the reported prevalence of metastases.
Results There was moderate but statistically significant correlation between BMC and metabolic activity ($r = 0.636$, $p < 0.0001$). Interestingly, the iliac and sacrum had higher metabolic activity relative to cellularity, whereas the femoral neck and lesser trochanter showed lower SUVr than other regions with the similar cellularity. The relatively lower metabolic status of the femoral neck conflicted with its reported high frequency of metastasis. Excluding regions with almost no remaining red marrow, cellularity showed inverse relationship with age ($r = 0.476$, $p < 0.0001$) and direct relationship with R2* ($r = 0.532$, $p < 0.0010$).
Conclusions Metabolic activity of bone marrow was largely dependent on BMC while yellow marrow seems metabolically quiescent. The discrepancy between the assumed vascularity as determined by metabolic activity and reported sites of metastasis suggested that the process of bone metastasis may not depend entirely on vascularity.

Keywords Positron emission tomography · Magnetic resonance imaging · PET/MR · Bone marrow · Metabolism · Metastasis

Introduction

Bone marrow is one of the largest organs in the body, and is composed of red marrow and yellow marrow [1]. Red marrow is responsible for hematopoiesis and is largely confined to the axial skeleton and proximal metaphysis of the long bones in adults [2]. Red marrow is more vascularized than yellow marrow [3, 4], and is the predominant site for hematogenous seeding of cancer cells [5–7]. Although at the current time the role of peripheral white or brown adipose tissue is fairly well understood, the function of yellow marrow remains somewhat cryptic [8]. Classically yellow marrow was thought to be quiescent tissue of limited metabolic importance [9]. A prior PET/MR study in cancer patients did not find metabolic activity in fatty marrow [10] but the relationship between cellularity and metabolic activity has not been studied. Also, red marrow, although considered more metabolically active, may become functionally quiescent to protect from “exhaustion” [11]. Hence, it might be important to determine the metabolic activity of normal subjects yellow and red marrow.

Metastases are felt to follow the distribution of the highly vascularized red marrow, although there is little information available about the metabolic activity of hematopoietic marrow [12]. Prior authors have suggested a correlation between metabolic activity and vascularity in normal bone and suggested the concept that metabolic activity could be used as biomarker assumption of vascularity [13, 14]. Because some red marrow is assumed to be more quiescent than others, the other component, fatty marrow could have variable metabolic activities.. Hence, better knowledge of the relationship

✉ Chuan Huang
chuan.huang@stonybrookmedicine.edu

[1] Department of Radiology, Stony Brook University, Stony Brook, NY, USA

[2] Department of Psychiatry, Stony Brook University, Stony Brook, NY, USA

between metabolic activity and the components of bone marrow is needed. This information in and of itself would be useful in understanding the biologic marrow activity and the relationship of this map with the distribution of metastasis.

PET/MR is useful for exploring bone marrow metabolism because of its simultaneous acquisition of metabolic activity and high tissue-contrast images. According to previous histological correlation [15], because of the high water content in hematopoietic cells, we can approximate bone marrow cellularity (BMC) through water fraction quantification with gradient echo images [16]. As has been shown with multiple studies in the liver, and other organs, multi-echo gradient echo sequences provide precise water–fat quantification by eliminating B_0 inhomogeneity effects from the surrounding trabecular network [17, 18].

Therefore, our purpose was to analyze the correlation between BMC determined from multi-echo gradient echo images and the metabolic activity of the pelvis and proximal femur in healthy subjects using PET/MR. We compared the results with tendencies of metastasis from published literature to clarify the contribution of metabolic activity to these tendencies. We also investigated the relationship between BMC and R2* values that suggested regional trabecular patterns.

Materials and methods

Subjects

This prospective study enrolled 11 consecutive volunteers (age = 39.3 ± 12, seven females) with no known cancer or marrow disorders who underwent PET/MR scans for other research protocols from March 2015 to November 2015. This prospective study was approved by institutional ethics committee and written informed consent was obtained from all subjects.

PET/MR examination

All subjects fasted overnight and were required to remain seated or recumbent to minimize glucose uptake in muscles after injection of the FDG (~5 mCi dose). One hour after injection, 10-min simultaneous 3-T PET/MR acquisitions of the pelvis and proximal femur were acquired on a Biograph mMR (Siemens Healthcare. Software version: VB20P). We used an 8-channel spinal coil and a 4-channel flexible surface coil. Both coils are dedicated PET/MR compatible coils provided by the vendor.

PET images reconstruction

PET images were reconstructed using a vendor-provided PSF-OSEM algorithm with three iterations and 21 subsets, 2.80-mm pixel spacing, and 2.03-mm thick slices. Attenuation correction was performed using a standard vendor-provided Dixon sequence. Mean standardized uptake values (SUV mean) were used to assess FDG uptake of bone marrow.

MR sequence

We measured apparent BMC through water–fat quantification with 3D Cartesian 6-echo gradient-echo pulse sequences (Fig. 1). The acquisition parameters were: 48 slices, acquisition matrix 192 × 126, pixel size = 2.08 × 2.08 mm^2, slice thickness/gapping = 4 mm/0 mm, flip angle = 6°, TR = 11 ms, six echoes with echo time = 1.37, 2.66, 4.92, 6.15, 7.33, 8.81 ms, 1 average, acquisition time = 1 min 40s, bandwidth = 1240 Hz/pixel. Water–fat signal separation was performed using a graph-cut algorithm with field inhomogeneity

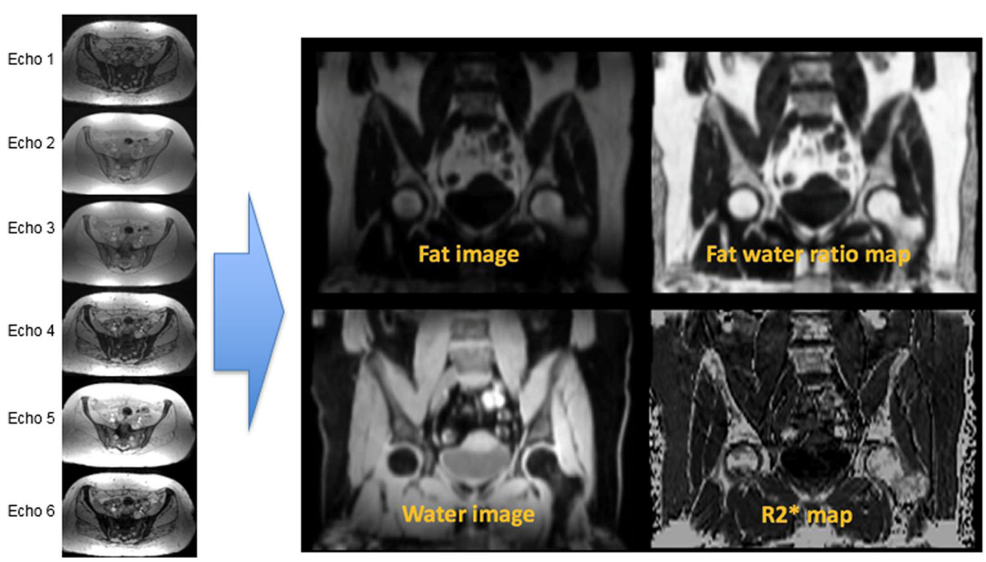

Fig. 1 Representative image of 6-echo Dixon sequence. Accurate fat–water ratio maps could be obtained to calculate precise bone marrow cellularity

and R2* correction using the magnitude and phase images based on a 6-peak fat-signal model [19].

Data analysis

As shown in Fig. 2, 20 (ten on each side) 1-cm^2 representative regions-of-interest (ROIs) were drawn manually in each subject on the corresponding axial PET and MR images using Osirix Lite 8.0 (Pixmeo SARL, Switzerland) in the sacral ala, iliac bone, ischium, acetabulum, pubic bone, femoral head, femoral neck, greater trochanter, lesser trochanter, and femoral subtrochanter by a musculoskeletal radiologist with 10 years of experience. The apparent water fraction for BMC and R2* in each ROI was extracted.

To standardize the SUV mean in each bone marrow site, we calculated the FDG SUV ratio (SUVr) normalized by the SUV in the gluteal muscle in each individual based on previous reports [20, 21].

Using the measured BMC and SUVr, we analyzed the symmetry of each parameter at the corresponding bilateral site. The expected inverse relationship between BMC and age was also analyzed. To look for any correlation between red marrow amount and metabolic activity—in other words, to show the yellow marrow is metabolically quiescent—we analyzed the correlation between BMC and SUVr of each site. We compared the relationship between BMC and SUVr with previously reported prevalence of bone metastasis among our evaluated sites. We also analyzed the relationship between BMC and R2*.

Statistical analysis

Pearson correlation was used to assess the correlation of BMC and SUVr between the bilateral marrow sites. We also used Pearson correlation to compare BMC and SUVr, age, and

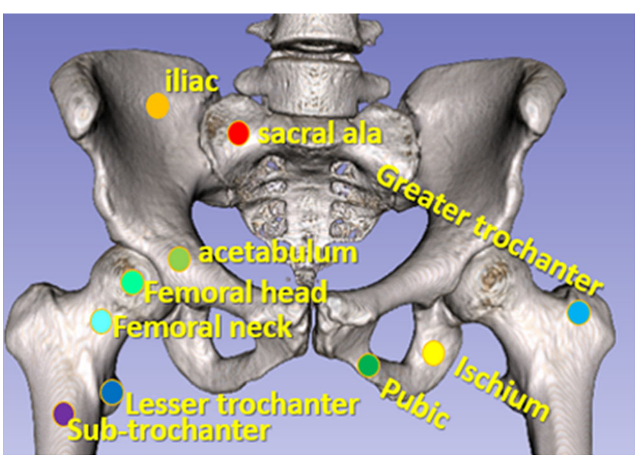

Fig. 2 ROIs used in this study. Volume rendering in 3D slicer using a separate CT volume as the reference standard

R2*. A p value less than 0.05 was considered statistically significant using SPSS.

Results

As shown in Fig. 3, the apparent BMC and SUVr has a fairly symmetrical distribution for each of the ROI pairs within individual subjects (correlation coefficient $r = 0.965$, $p < 0.0001$ for cellularity, and $r = 0.960$, $p < 0.0001$ for SUVr).

Excluding the femoral head and greater trochanter, where almost complete conversion to yellow marrow had already occurred, there was an inverse correlation between BMC and age ($r = 0.476$, $p < 0.0001$) as in Fig. 4. The inverse correlation at each region was also confirmed graphically (data not shown) but we did not analyze each region because the number of subjects was too small.

Figure 5 shows a moderate but statistically significant linear correlation between marrow cellularity and its corresponding SUVr ($r = 0.636$, $p < 0.0001$). This suggests that the metabolic activity of bone marrow is regulated by its cellularity. Of all the sites, we found the highest ratio of SUVr to BMC in the sacrum and iliac in the pelvic ring. While the neck and lesser trochanter of the femur had the lowest ratio of SUVr to BMC.

Data from the Rizzoli Institute regarding the first locations of 4110 metastatic bone tumors showed the high incidence as 12.6% for the iliac bones and 3.4% for the sacrum in axial skeleton [22]. These are the same areas of bone marrow with high FDG uptake to cellularity in our study. The Rizzoli data showed a high prevalence of metastatic tumors in the proximal femur (20.4%) and it has also been reported that half of femoral metastases occur in the femoral neck [23]. However, our results showed less metabolic activity in the femoral neck despite the presence of a fair amount of BMC.

The relationship between BMC and R2* is shown in Fig. 6. Combining data from the pelvis, femoral neck, lessor trochanter, and femoral subtrochanter showed a moderate direct correlation ($r = 0.532$, $p < 0.0010$), but the R2* values in the femoral head and greater trochanter varied despite their consistently low cellularity ($r = 0.583$, $p = 0.0044$).

Discussion

Bone marrow biopsy is still regarded as the gold standard for bone marrow evaluation. It is, however, invasive and uncomfortable for the patient and produces only a small geographically limited sample. Both PET and MRI have been shown to be promising methods to provide quantitative assessment of bone marrow. Using simultaneous PET/MR allows one to potentially match several indicators of marrow metabolic

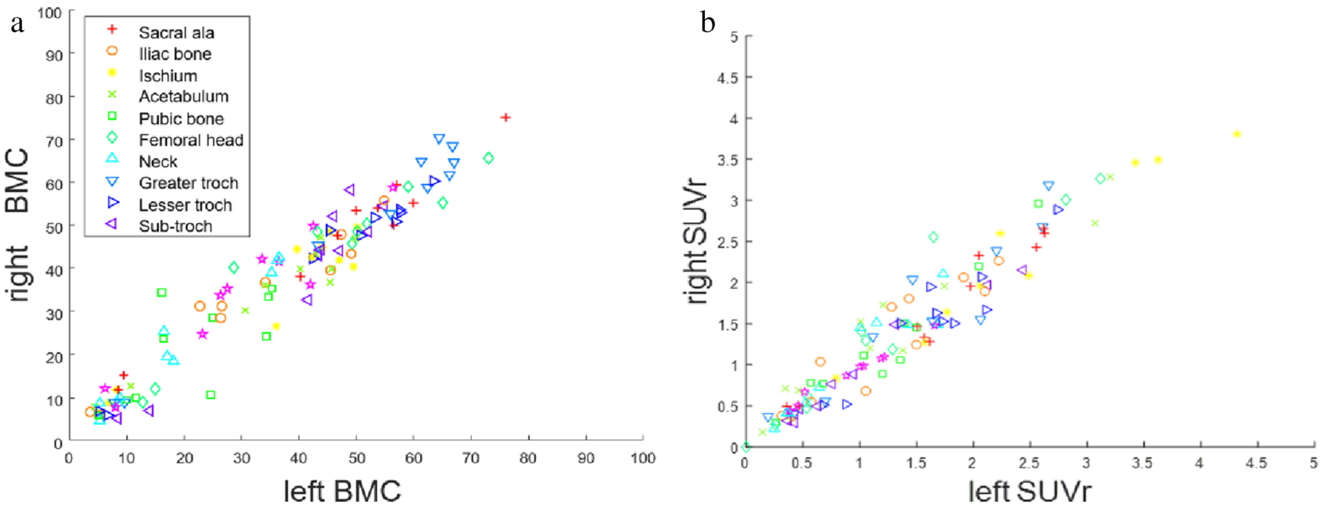

Fig. 3 Symmetry of bone marrow cellularity and SUVr between the left and right ROIs. There was strong symmetricity with correlation coefficients of $r = 0.965$ in bone marrow cellularity (**a**) and $r = 0.950$ in SUVr (**b**)

activity, as FDG-PET scans provide in vivo semi-quantitative assessment of glucose metabolism by evaluating FDG uptake [24] and MR imaging enables differentiation of the two types of bone marrow with high tissue contrast resolution [1].

Yellow marrow has fewer hematopoietic components and composition of more than 80% fat [2]. It yields higher signal intensity than skeletal muscle on T1-weighted images. Even though red marrow shows lower signal intensity than subcutaneous fat on T1-weighted images, the signal is still higher than skeletal muscle, due a fat fraction of 40% [2]. Because fat is a major component even in red marrow, and MR is sensitive to fat, a small amount of hematopoietic cells may not be morphologically evaluable on conventional T1-weighted images [25], marrow cellularity might be a more accurate measure of the non-fatty components of bone marrow and might be a window into nonquiescent marrow.

Water and fat can be effectively separated on MR by using "in- and out of phase" imaging, which was first described by Dixon in 1984 [16]. In this study, we used a multi-echo gradient echo technique to measure marrow cellularity as it is known that water–fat quantification by two-point DIXON is affected by the trabecular network because of B_0 inhomogeneity [26], as well as R2* decay. This multi-echo gradient echo is the optimal method to evaluate the cellular and the R* values, the trabecular aspects of marrow. Acquiring this data, concurrently with FDG PET provides additional metabolic data [27].

Fig. 4 Relationship between marrow cellularity and age. An inverse relationship was found, excluding femoral head and greater trochanter

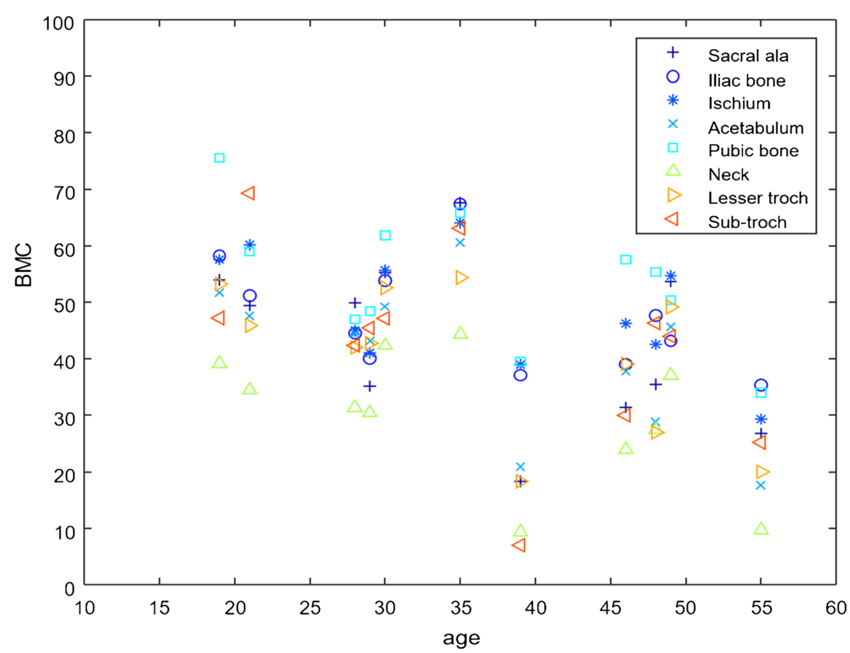

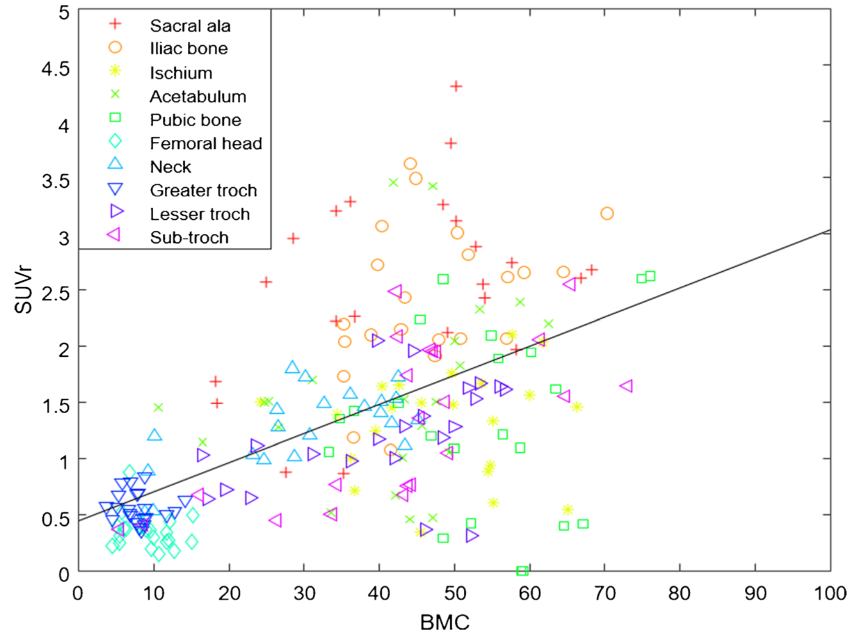

Fig. 5 Correlation between SUVr and bone marrow cellularity (BMC). Direct linear correlation was shown with correlation coefficient of $r = 0.636$

It is well known that physiologic conversion from red to yellow marrow occurs in a symmetrical and predictable sequence [1]. Our results mirrored these known relationships between BMC and age. Our results also showed that the femoral head and greater trochanter of the femur had the lowest cellularity among the evaluated sites, again as expected [28], and also showed the least FDG uptake. Sambuceti et al. suggested a threshold SUV of 1.11 to differentiate red and yellow marrow on PET/CT [29]. Red marrow is known to contain approximately 60% hematopoietic cells [30], concordant with our results. Our observation of cellularity and SUVr showed that 60% cellularity approximated an SUVr of around 1.0. We also have shown that BMC and metabolic activity were symmetrically distributed, as has been noted previously using alternate methodologies [1, 24].

We found that the metabolic activity of bone marrow correlated with BMC, which suggests that the metabolic activity of bone marrow depends on the amount of cellularity. This also implied that bone marrow adipose tissue, which is dominant in yellow marrow, is metabolically quiescent. Previously, Schraml et al. investigated the relationship between fat fraction with two-point DIXON and FDG uptake in cancer patients [10]. They showed an inverse correlation of fat fraction and FDG uptake in bone marrow, which could be considered to parallel our results. Because our subjects were free from cancer or chemoradiation therapy, and we used a multi-echo gradient echo technique to more accurately measure the water–fat composition, our results are based on normal bone marrow function with more precise hematopoietic component quantification, than any prior study.

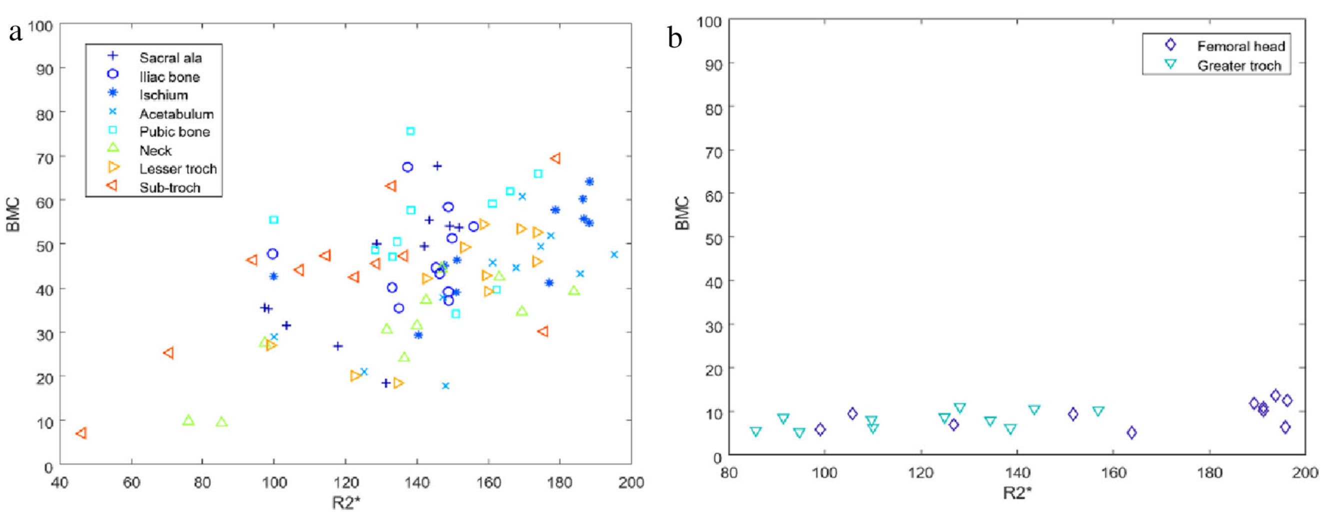

Fig. 6 Relationship between BMC and R2*. A direct linear correlation was found in the pelvis and femur, but excluding the femoral head and greater trochanter (**a**). Excluded regions showed variable R2* regardless of consistently low marrow cellularity (**b**)

When looking at the relationship between BMC and metabolic activity, some parts of the bone marrow had relatively higher or lower metabolic activity rates even with similar cellularity values. The sacrum and iliac had relatively high SUVr, while the femoral neck and lesser trochanter of femur had relatively low SUVr even though they all had similar measured cellularity. Although this could also be in part due to imperfect attenuation correction provided by the vendor, our results suggest interesting information that the metabolic activity of hematopoietic cells might vary by location.

If we assume that marrow with high levels of metabolic activity are also more highly vascularized, we could postulate that these areas with high metabolic activity would naturally indicate areas of potential tumor seeding, since the distribution of bone metastases is usually explained by the high vascularity in red marrow [4]. However, this conjecture did not perfectly agree with epidemiological data of bone metastasis. Among femur bone metastases, half occur in the femoral neck followed by subtrochanteric and intertrochanteric sites [23] but our results showed that red marrow in the femoral neck had relatively low metabolic activity, which is conjectured to reflect vascularity. Although the static FDG uptake we used to estimate vascularity was not a direct measurement of vascularity and some caution should be needed for its interpretation, our finding suggested that the process of bone metastasis might not be explained by vascularity alone. In fact, despite its clinical importance, the mechanism of tumor metastasis is not well understood. Historically, the "seed and soil" theory by Paget [31] has gained acceptance as a basic principle of metastatic spread, displacing the hemodynamic theory. The theory proposes that tumor cells are able to survive and grow in specific microenvironments in specific organs and are not ruled only by vascularity [32]. In our results, the bone marrow metabolic activity, an indication of vascularity, did not perfectly correlate with the reported metastatic tendency, which may suggest that the process of metastasis could be more complicated than simple tissue vascularity. Consequently, further studies are needed to better understand why red marrow is specifically a good soil for metastasis. However, even though a parallel relationship between glucose uptake and blood flow was suggested in normal bone tissue previously [13, 14], glucose metabolism is not a direct measurement of vascularity. Also, this study was not guaranteeing the utility of static FDG uptake for vascularity assumption in other organs or cancer tissues. Therefore, exploring the relationship between direct assessment of vascularity with dynamic contrast enhancement or dynamic NaF-PET scan and metabolic status or marrow cellularity would be necessary and helpful for further understanding of these complex interactions.

Because R2* values can also be generated using the multi-echo gradient echo technique, we evaluated the relationship of BMC and R2*. It is known that the R2* value decreases in osteoporosis [33, 34]. Our results showed that there was positive correlation between cellularity and R2* values in the pelvis and femur except for the femoral head and greater trochanter. This may indirectly suggest a decrease in the hematopoietic component in osteoporotic bone marrow, as had been previously suggested [34]. The femoral head and greater trochanter, however, showed a variety of R2* values despite their consistently low cellularity. The reason is not clear but because the R2* value is dependent on the orientation of the trabecula relative to the polarizing field [35], the value could vary in some parts of the femur due to rotation or abduction while in the scanner. In addition, the femoral head can have a variety of subchondral changes, which can cause susceptibility effects due to weight-loading articulation. These factors together can make it hard to perform a reliable R2* evaluation.

Several limitations in this preliminary study should be acknowledged. First, the sample size is relatively small. Our subjects, however, were all healthy volunteers and the necessity of radiation exposure precluded ethically including more subjects. To compensate, we evaluated multiple sites in each individual to maximize the amount of data we could obtain from the limited number of subjects. In addition, because the majority of PET/MR studies were not conducted with healthy volunteers, we believe our study can provide new insight about normal bone marrow function. Secondly, we used the data of healthy subjects from another prospective study, so the age, sex, smoking history, and obesity of the subjects were not balanced. Although, sex has little potential to affect bone marrow function [29], age should have a critical effect and our subjects were relatively young. A young population, however, could be more suitable for examining the relationship between bone marrow metabolism and marrow cellularity because red marrow converts to yellow with age. Smoking history and obesity were the factors that could potentially affect marrow function, thereby, it should be balanced in any future studies. Thirdly, accurate attenuation correction of bone regions in PET/MR is still challenging, and the vendor-provided attenuation correction used here was suboptimal. An underestimation of SUV quantification in bone of as much as 14% was reported previously [36]. However, all the bone regions should be similarly underestimated and we believe there was little effect on our correlation analysis. This limitation was accepted in a previous PET/MR study for bone marrow including pelvis and femur [10]. Fourthly, a similar dose of 5 mCi was used for all subjects. The dose should be optimized depending on the weight, but a relative small dose was only approved by our IRB. Lastly, we performed cross-sectional analysis but longitudinal analysis would be more helpful to understand our results and make them more reliable.

In conclusion, metabolic activity of bone marrow in healthy subjects was correlated with the amount of BMC, and the adipose tissue that is dominant in yellow marrow could be regarded as metabolically quiescent. Furthermore, while the sacrum and iliac bones showed relatively higher metabolic rates than other bones at the same cellularity, the femoral neck and lesser trochanter of the femur showed lower rates. Because metabolic activity could be assumed to reflect vascularity in normal marrow, we compared this tendency with the previously reported frequency of bone metastasis and found they did not perfectly agree. This suggests that the process of bone metastasis may not depend solely on vascularity. However, as metabolic activity is not a direct measure of vascularity, further studies are required to validate the findings of this preliminary study.

Compliance with ethical standards

Conflict of interest The authors declare that they have no conflicts of interest.

Ethical approval All procedures performed in studies involving human participants were in accordance with the ethical standards of the institutional research committee and with the 1964 Helsinki Declaration and its later amendments or comparable ethical standards.

Informed consent Informed consent was obtained from all individual participants included in the study.

References

1. Hwang S, Panicek DM. Magnetic resonance imaging of bone marrow in oncology, part 1. Skelet Radiol. 2007;36(10):913–20.
2. Navarro SM, Matcuk GR, Patel DB, Skalski M, White EA, Tomasian A, et al. Musculoskeletal imaging findings of hematologic malignancies. Radiographics. 2017;37(3):881–900.
3. Basu S, Houseni M, Bural G, Chamroonat W, Udupa J, Mishra S, et al. Magnetic resonance imaging based bone marrow segmentation for quantitative calculation of pure red marrow metabolism using 2-deoxy-2-[F-18]fluoro-D-glucose-positron emission tomography: a novel application with significant implications for combined structure-function approach. Mol Imaging Biol. 2007;9(6): 361–5.
4. Budzik JF, Lefebvre G, Forzy G, El Rafei M, Chechin D, Cotten A. Study of proximal femoral bone perfusion with 3D T1 dynamic contrast-enhanced MRI: a feasibility study. Eur Radiol. 2014;24(12):3217–23.
5. Krishnamurthy GT, Tubis M, Hiss J, Blahd WH. Distribution pattern of metastatic bone disease. A need for total body skeletal image. JAMA. 1977;237(23):2504–6.
6. Tubiana-Hulin M. Incidence, prevalence and distribution of bone metastases. Bone. 1991;12(Suppl 1):S9–10.
7. Choi J, Raghavan M. Diagnostic imaging and image-guided therapy of skeletal metastases. Cancer control. 2012;19(2):102–12.
8. Hardouin P, Rharass T, Lucas S. Bone marrow adipose tissue: to be or not to be a typical adipose tissue? Front Endocrinol (Lausanne). 2016;7:85.
9. Krings A, Rahman S, Huang S, Lu Y, Czernik PJ, Lecka-Czernik B. Bone marrow fat has brown adipose tissue characteristics, which are attenuated with aging and diabetes. Bone. 2012;50(2):546–52.
10. Schraml C, Schmid M, Gatidis S, Schmidt H, la Fougere C, Nikolaou K, et al. Multiparametric analysis of bone marrow in cancer patients using simultaneous PET/MR imaging: correlation of fat fraction, diffusivity, metabolic activity, and anthropometric data. J Magn Reson Imaging. 2015;42(4):1048–56.
11. Nakamura-Ishizu A, Takizawa H, Suda T. The analysis, roles and regulation of quiescence in hematopoietic stem cells. Development. 2014;141(24):4656–66.
12. Suva LJ, Washam C, Nicholas RW, Griffin RJ. Bone metastasis: mechanisms and therapeutic opportunities. Nat Rev Endocrinol. 2011;7(4):208–18.
13. Lafage-Proust MH, Roche B, Langer M, Cleret D, Vanden Bossche A, Olivier T, et al. Assessment of bone vascularization and its role in bone remodeling. Bonekey rep. 2015;4:662.
14. Heinonen I, Kemppainen J, Kaskinoro K, Langberg H, Knuuti J, Boushel R, et al. Bone blood flow and metabolism in humans: effect of muscular exercise and other physiological perturbations. J Bone Miner Res. 2013;28(5):1068–74.
15. MacEwan IJ, Glembotski NE, D'Lima D, Bae W, Masuda K, Rashidi HH, et al. Proton density water fraction as a biomarker of bone marrow cellularity: validation in ex vivo spine specimens. Magn Reson Imaging. 2014;32(9):1097–101.
16. Dixon WT. Simple proton spectroscopic imaging. Radiology. 1984;153(1):189–94.
17. Reeder SB, McKenzie CA, Pineda AR, Yu H, Shimakawa A, Brau AC, et al. Water–fat separation with IDEAL gradient-echo imaging. J Magn Reson Imaging. 2007;25(3):644–52.
18. Ma J. Dixon techniques for water and fat imaging. J Magn Reson Imaging. 2008;28(3):543–58.
19. Hernando D, Kellman P, Haldar JP, Liang ZP. Robust water/fat separation in the presence of large field inhomogeneities using a graph cut algorithm. Magn Reson Med. 2010;63(1):79–90.
20. Gheysens O, Postnov A, Deroose CM, Vandermeulen C, de Hoon J, Declercq R, et al. Quantification, variability, and reproducibility of basal skeletal muscle glucose uptake in healthy humans using 18F-FDG PET/CT. J Nucl Med. 2015;56(10):1520–6.
21. Tsujikawa T, Tsuyoshi H, Kanno M, Yamada S, Kobayashi M, Narita N, et al. Selected PET radiomic features remain the same. Oncotarget. 2018;9(29):20734–46.
22. Picci P, Manfrini M, Fabbri N, Gambarotti M, Vanel D. Atlas of musculoskeletal tumors and tumorlike lesions. The Rizzoli case archive. Berlin: Springer; 2014. p. 251–2.
23. Feng H, Wang J, Xu J, Chen W, Zhang Y. The surgical management and treatment of metastatic lesions in the proximal femur: a mini review. Medicine (Baltimore). 2016;95(28):e3892.
24. Yao WJ, Hoh CK, Hawkins RA, Glaspy JA, Weil JA, Lee SJ, et al. Quantitative PET imaging of bone marrow glucose metabolic response to hematopoietic cytokines. J Nucl Med. 1995;36(5):794–9.
25. Vande Berg BC, Lecouvet FE, Galant C, Simoni P, Malghem J. Normal variants of the bone marrow at MR imaging of the spine. Semin Musculoskelet Radiol. 2009;13(2):87–96.
26. Hernando D, Haldar JP, Sutton BP, Ma J, Kellman P, Liang ZP. Joint estimation of water/fat images and field inhomogeneity map. Magn Reson Med. 2008;59(3):571–80.
27. Rosenkrantz AB, Friedman K, Chandarana H, Melsaether A, Moy L, Ding YS, et al. Current status of hybrid PET/MRI in oncologic imaging. AJR Am J Roentgenol. 2016;206(1):162–72.
28. Moore SG, Dawson KL. Red and yellow marrow in the femur: age-related changes in appearance at MR imaging. Radiology. 1990;175(1):219–23.
29. Sambuceti G, Brignone M, Marini C, Massollo M, Fiz F, Morbelli S, et al. Estimating the whole bone-marrow asset in humans by a computational approach to integrated PET/CT imaging. Eur J Nucl Med Mol Imaging. 2012;39(8):1326–38.
30. Vande Berg BC, Malghem J, Lecouvet FE, Maldague B. Magnetic resonance imaging of the normal bone marrow. Skelet Radiol. 1998;27(9):471–83.
31. Paget S. The distribution of secondary growths in cancer of the breast. 1889. Cancer Metastasis Rev. 1989;8(2):98–101.
32. Fidler IJ. The pathogenesis of cancer metastasis: the 'seed and soil' hypothesis revisited. Nat Rev Cancer. 2003;3(6):453–8.

33. Wehrli FW, Ford JC, Haddad JG. Osteoporosis: clinical assessment with quantitative MR imaging in diagnosis. Radiology. 1995;196(3):631–41.
34. Baum T, Yap SP, Karampinos DC, Nardo L, Kuo D, Burghardt AJ, et al. Does vertebral bone marrow fat content correlate with abdominal adipose tissue, lumbar spine bone mineral density, and blood biomarkers in women with type 2 diabetes mellitus? J Magn Reson Imaging. 2012;35(1):117–24.
35. Song HK, Wehrli FW, Ma J. Field strength and angle dependence of trabecular bone marrow transverse relaxation in the calcaneus. J Magn Reson Imaging. 1997;7(2):382–8.
36. Hofmann M, Bezrukov I, Mantlik F, Aschoff P, Steinke F, Beyer T, et al. MRI-based attenuation correction for whole-body PET/MRI: quantitative evaluation of segmentation- and atlas-based methods. J Nucl Med. 2011;52(9):1392–9.